



Bai, X., Bessa, M. A., Melro, A. R., Camanho, P., Guo, L., & Liu, W. K. (2016). Erratum: Corrigendum to “High-fidelity micro-scale modeling of the thermo-visco-plastic behavior of carbon fiber polymer matrix composites” (Composite Structures (2015) 134 (132–141)). *Composite Structures*, 153, 724-727. <https://doi.org/10.1016/j.compstruct.2016.05.081>

Peer reviewed version

License (if available):
CC BY-NC-ND

Link to published version (if available):
[10.1016/j.compstruct.2016.05.081](https://doi.org/10.1016/j.compstruct.2016.05.081)

[Link to publication record in Explore Bristol Research](#)
PDF-document

This is the accepted author manuscript (AAM). The final published version (version of record) is available online via Elsevier at <http://dx.doi.org/10.1016/j.compstruct.2016.05.081>. Please refer to any applicable terms of use of the publisher.

University of Bristol - Explore Bristol Research

General rights

This document is made available in accordance with publisher policies. Please cite only the published version using the reference above. Full terms of use are available:
<http://www.bristol.ac.uk/pure/about/ebr-terms>

Corrigendum: High-fidelity micro-scale modeling of the thermo-visco-plastic behavior of carbon fiber polymer matrix composites

Xiaoming Bai^{a,b}, Miguel A. Bessa^b, António R. Melro^c, Pedro P. Camanho^{d,e},
Licheng Guo^{a,2,*}, Wing Kam Liu^{b,1,*}

^a*Department of Astronautic Science and Mechanics, Harbin Institute of Technology,
Harbin, P.R. China 150001*

^b*Department of Mechanical Engineering, Northwestern University, 2145 Sheridan Rd.,
Evanston, IL 60201, U.S.A.*

^c*Advanced Composites Centre for Science and Innovation (ACCIS), University of Bristol,
Queen's Building, University Walk, Bristol BS8 1TR, UK*

^d*DEMec, Faculdade de Engenharia, Universidade do Porto, Rua Dr. Roberto Frias,
4200-465, Porto, Portugal*

^e*INEGI, Rua Dr. Roberto Frias, 400, 4200-465 Porto, Portugal*

Abstract

The authors would like to inform that one of the modifications proposed in the article “High-fidelity micro-scale modeling of the thermo-visco-plastic behavior of carbon fiber polymer matrix composites” [1] was found to be unnecessary: the paraboloid yield criterion is sufficient to describe the shear behavior of the epoxy matrix considered (Epoxy 3501-6). The authors recently noted that the experimental work [2] used to validate the pure matrix response considered engineering shear strain instead of its tensorial counter-part, which caused the apparent inconsistency with the paraboloid yield criterion.

A recently proposed temperature dependency law for glassy polymers is evaluated herein and better agreement with the experimental results for this epoxy is observed.

1. Unnecessary modification of paraboloid yield criterion

Werner and Daniel [2] considered engineering shear strain in the experimental stress-strain curve provided for the epoxy resin 3501-6, instead of its tensorial counter-part. Taking this into consideration, Figure 1(a) demonstrates that the shear prediction for the unmodified paraboloid yield criterion (Eq. (1) in the original article [1]) is in fact in good agreement with the experimental shear behavior of the epoxy matrix. Therefore, the authors recommend to ignore the

*Corresponding author

¹w-liu@northwestern.edu

²guolc@hit.edu.cn

proposed modification to the yield criterion, i.e. Eqs. (2-5) and Appendix A in [1], since the correction for shear is minimal and does not lead to a significant improvement in the predictions of the composite response.

The unmodified paraboloidal yield criterion [3, 4] can thus be written as:

$$f(\boldsymbol{\sigma}, \sigma_{Y_C}, \sigma_{Y_T}) = 6J_2 + 2(\sigma_{Y_C} - \sigma_{Y_T}) I_1 - 2\sigma_{Y_C}\sigma_{Y_T} \quad (1)$$

where σ_{Y_C} and σ_{Y_T} are the absolute values of compressive and tensile yield stresses, $I_1 = \text{tr}(\boldsymbol{\sigma}_{ij})$ is the first stress invariant, and $J_2 = \frac{1}{2}\boldsymbol{s}_{ij}\boldsymbol{s}_{ij}$ is the second invariant of the deviatoric stress tensor \boldsymbol{s}_{ij} .

The authors note that the epoxy constitutive model using the unmodified paraboloid criterion only requires the input of two hardening laws instead of the three needed previously (since the shear curve is no longer needed). Table 1 shows the input parameters for the model at room temperature (25 °C), where the units for the Young’s modulus E and yield stresses σ_{Y_n} are in MPa ($n = T$ for tension and $n = C$ for compression). It is clarified that the hardening laws are inputted as tabular values respectively from the tensile and compressive experimental response after the stress reaches $\sigma_{Y_T} \approx 3.3$ MPa and $\sigma_{Y_C} \approx 58.0$ MPa. These values of σ_{Y_T} and σ_{Y_C} are lower than previously reported [1] in order to better replicate the experimental curves, but this choice does not have significant influence since the nonlinearity until the previously reported values is small.

Recall that the material constants α_n are used in the hardening laws and are related to the strain-rate dependency of the material as defined previously in the original article [1], see also Eq. (3) included herein. These material constants are determined experimentally by scaling back to the reference state each stress-strain curve that is obtained for the different strain-rates. Therefore, the previous calibration of α_n parameters affecting the strain-rate dependence was verified to be appropriate.

Figures 1(a) and 1(b) show the calibrated response for tension and compression under quasi-static loads, as well as the predicted response for multiple strain-rates in (b). Figure 2 shows the prediction for the compression with torsion test, where it is clear that the paraboloid yield criterion is sufficient.

Table 1: Input parameters for the Epoxy 3501-6 matrix constitutive model. (Experimental results from Werner and Daniel [2])

E	ν	ν_p	σ_{Y_C}	σ_{Y_T}	α_C	α_T	β_C	β_T
4600	0.34	0.3	58.0	3.3	0.042	0.0	-	-

2. An update to the epoxy’s temperature dependence

Recently, some of the co-authors conducted fully atomistic analyses [5] of an epoxy polymer to determine the temperature dependence of the elastic modulus

(see Eq. (1) in [5]) and yield stresses (see Eq. (14) in [5]). Considering this update when describing the temperature dependence of the Epon 862 evaluated in [1] is shown to lead to better predictions.

The elastic modulus is then defined as [5]:

$$\ln\left(\frac{E^*}{E(T)}\right) = \theta (T - T^*) \quad (2)$$

where θ is the Young's modulus temperature dependence parameter determined from atomistic simulations, the superscript * indicates reference values, as before, and the yield stresses used in the hardening law can be modified to the simpler relationship [5]:

$$\sigma_{Y_n} = \sigma_{Y_n}^* \left(1 + \alpha_n \ln \frac{\dot{\varepsilon}_e^p}{\dot{\varepsilon}_e^{p*}}\right) + \beta_n (T - T^*) \quad (3)$$

where β_n are the temperature dependence parameters of the hardening laws in tension ($n = T$) and compression ($n = C$), α_n are the strain-rate dependence parameters, and $\dot{\varepsilon}_e^p$ represents the equivalent plastic strain rate. The material parameters obtained for the Epon 862 epoxy considering the above hardening laws are summarized in Table 2. The units for the Young's modulus E^* and yield stresses σ_{Y_n} are in MPa.

Table 2: Input parameters for the Epon 862 epoxy constitutive model. (Experimental results from Poulain *et al.* [6] at a reference temperature of 25 °C)

E^*	θ	ν	ν_p	σ_{Y_C}	σ_{Y_T}	α_C	α_T	β_C	β_T
2600	0.0048	0.4	0.3	68.12	48.64	0.035	0.035	-0.62	-0.62

Figure 3 shows the response obtained for the Epon 862 epoxy for different temperatures and strain rates for both tensile and compressive loads. A better prediction can be observed according to the updated temperature dependence. In addition, according to Vu-bac *et al.* [5] every parameter in Table 2 can be determined from molecular dynamics simulations, with the exception of α_n that describe the strain-rate dependency of the material.

3. Composite material response

The composite material (AS4/3501-6) response obtained with the paraboloid criterion for different loading conditions is shown in Figures 4 and 5. The average stress-strain response of the RVE subjected to transverse compression for the strain rate of 10^{-4} s^{-1} and 380 s^{-1} are shown in Figure 4. Good agreement with the experiment at a strain rate of 10^{-4} s^{-1} is observed. The experimental curve at a strain rate of 380 s^{-1} shows a visco-elastic effect, since the elastic modulus is slightly greater than the one measured for a strain rate of 10^{-4} s^{-1} .

However, the pure matrix experimental results reported by Werner and Daniel [2] and shown in Figure 1(b) do not show a clear visco-elastic effect. Also, according to Soden *et al.* [7], the AS4 carbon fibers are not expected to show a visco-elastic effect. Additional experiments should be conducted to clarify the source of visco-elasticity of the composite for this loading condition.

Finally, Figure 5 shows the result for the 45° off-axial compression test for a cubic RVE with length $l = 48 \mu\text{m}$, using non-periodic boundary conditions and modeling directly the orientation of the fibers. This result also indicates that the model with the paraboloid criterion is sufficient to predict the response of the composite material for this loading condition. Appendix B in [1] can be disregarded. Future work will be conducted in order to assess the influence of matrix and fiber damage on the composite response, as well as the influence of microstructural imperfections such as fiber waviness.

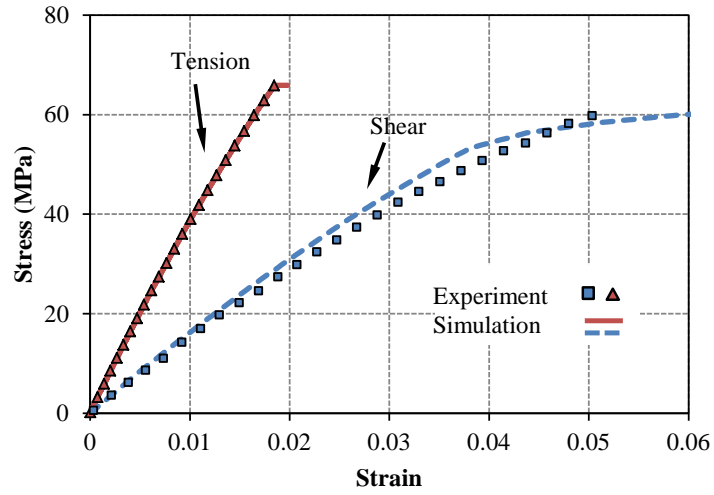
4. Conclusion

The modification of the paraboloid yield criterion proposed in the author's previous article [1] is unnecessary, since the correction for shear is minimal and does not lead to a significant improvement of the predicted composite response. The authors took the opportunity to validate a new temperature dependence law proposed recently by Vu-Bac *et al.* [5] and better agreement with the experimental results was observed. The paraboloid criterion and the updated thermal dependence laws for the epoxy matrix constitutive behavior can be obtained from atomistic simulations, without experimental input as in [5].

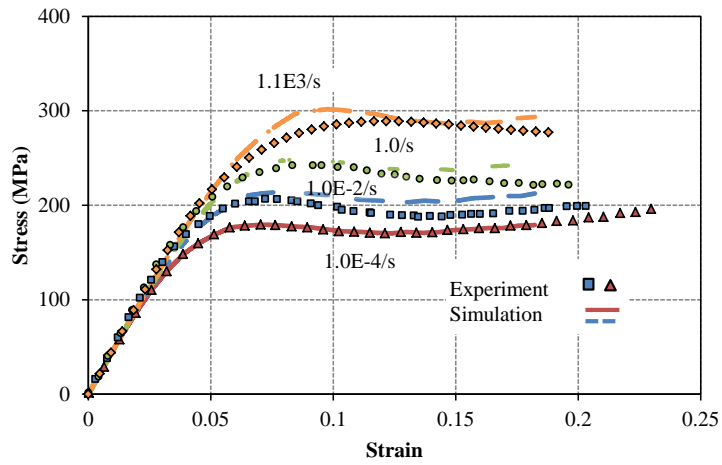
References

- [1] X. Bai, M. A. Bessa, A. R. Melro, P. P. Camanho, L. Guo, W. K. Liu, High-fidelity micro-scale modeling of the thermo-visco-plastic behavior of carbon fiber polymer matrix composites, *Composite Structures* 134 (2015) 132–141.
- [2] B. Werner, I. Daniel, Characterization and modeling of polymeric matrix under multi-axial static and dynamic loading, *Compos Sci Technol* 102 (0) (2014) 113 – 119.
- [3] N. W. Tschoegl, Failure surfaces in principal stress space, *J Polym Sci Polym Sym* 32 (1) (1971) 239–267.
- [4] A. Melro, P. Camanho, F. A. Pires, S. Pinho, Micromechanical analysis of polymer composites reinforced by unidirectional fibres: Part I - Constitutive modelling, *Int J Solids Struct* 50 (11–12) (2013) 1897 – 1905.
- [5] N. Vu-Bac, M. Bessa, T. Rabczuk, W. Liu, A multiscale model for the quasi-static thermo-plastic behavior of highly cross-linked glassy polymers, *Macromolecules* 48 (18) (2015) 6713–6723.
- [6] X. Poulain, A. Benzerga, R. Goldberg, Finite-strain elasto-viscoplastic behavior of an epoxy resin: Experiments and modeling in the glassy regime, *Int J Plast* 62 (0) (2014) 138 – 161.
- [7] P. Soden, M. Hinton, A. Kaddour, Lamina properties, lay-up configurations and loading conditions for a range of fibre-reinforced composite laminates, *Compos Sci Technol* 58 (7) (1998) 1011 – 1022.

- [8] I. Daniel, B. Werner, J. Fenner, Strain-rate-dependent failure criteria for composites, *Compos Sci Technol* 71 (3) (2011) 357 – 364.



(a) Uniaxial tension and shear test.



(b) Uniaxial compression test.

Figure 1: Calibration of the polymeric matrix constitutive model for epoxy 3501-6. Experimental results from [2].

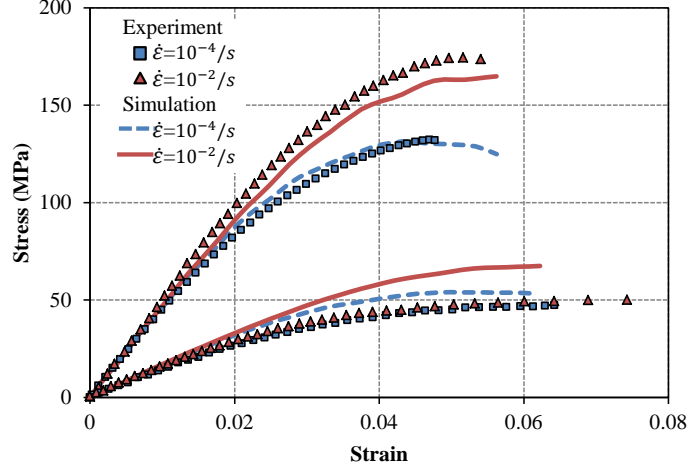
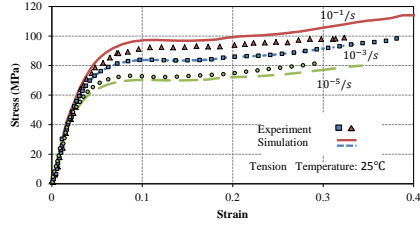
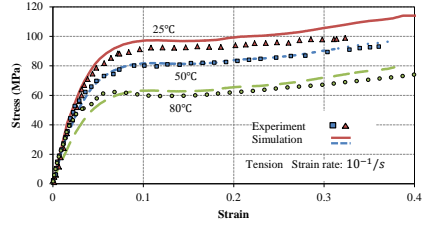


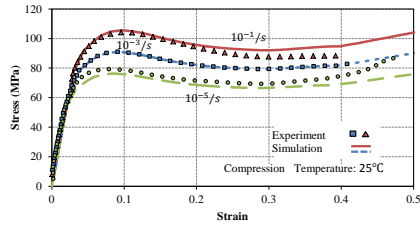
Figure 2: Matrix constitutive model prediction for epoxy 3501-6 under a combined load of compression and torsion. Experimental results from [2].



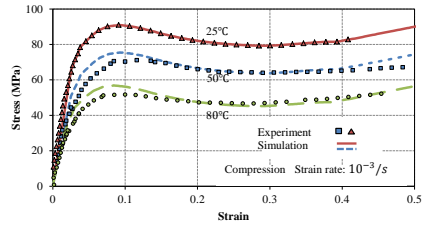
(a) Tension under different strain-rates



(b) Tension at different temperatures



(c) Compression under different strain-rates



(d) Compression at different temperatures

Figure 3: Calibration of the polymeric matrix constitutive model for the Epon 862 epoxy. Experimental results from [6].

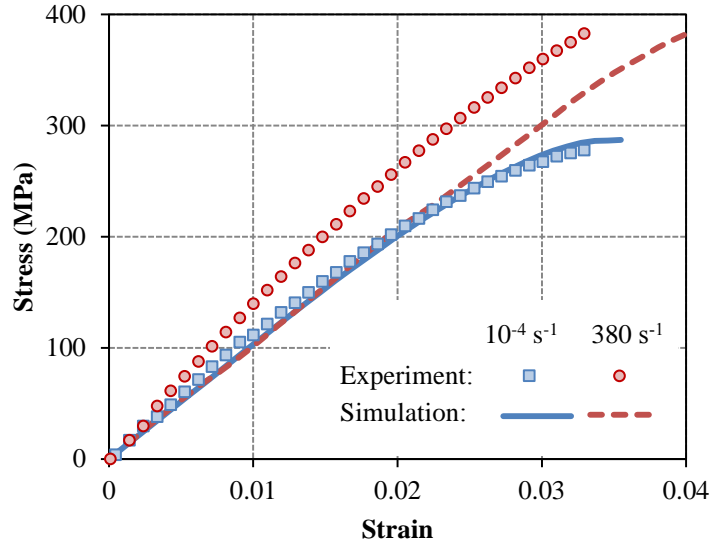


Figure 4: Comparison of experiment and present model for transverse compression. Experimental results from [8].

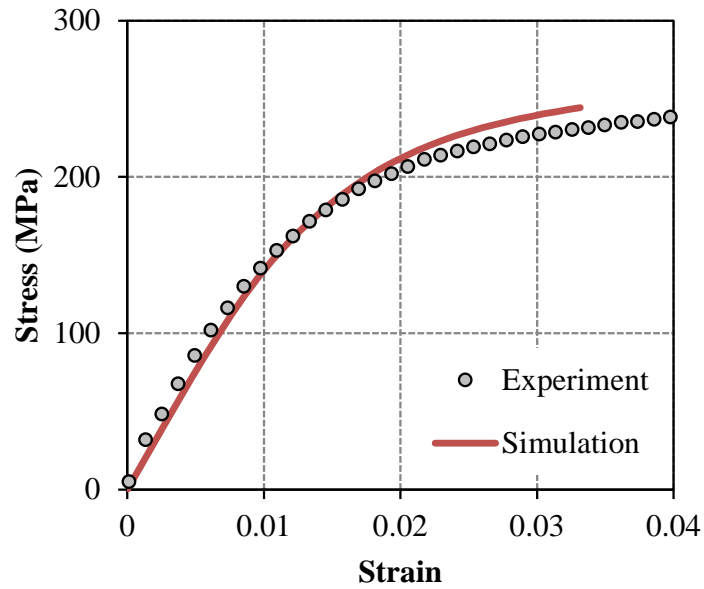


Figure 5: Comparison of experiment and present model for 45° off axial shear. (Strain rate: 10^{-4} s^{-1}). Experimental results from [8].